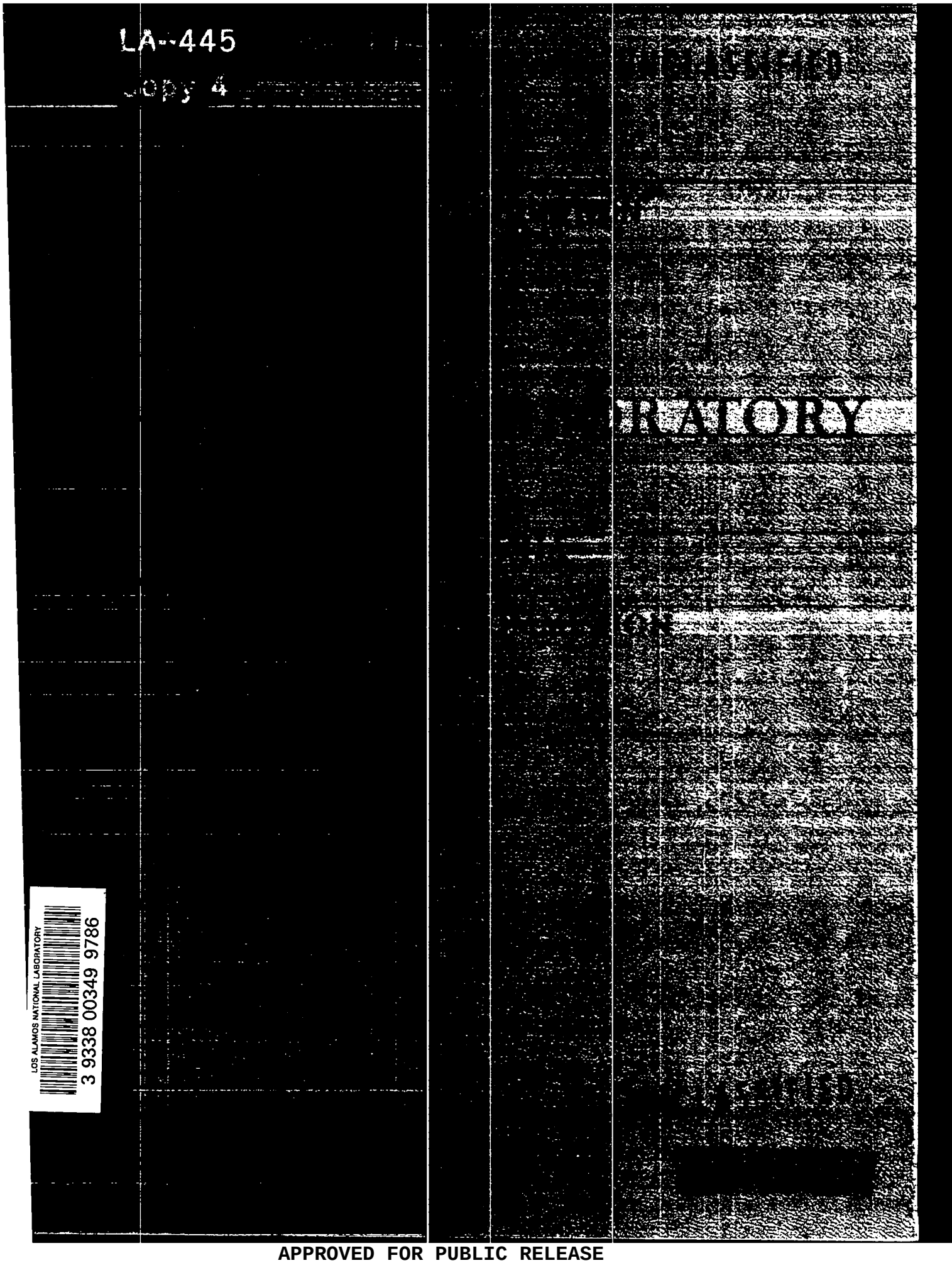

UNCLASSIFIED

[redacted]

LA-445

[redacted]

November 3, 1945 This document contains 40 pages

FISSION CROSS SECTIONS BY THE Be^7 AND Mn-BATH METHODS

WORK DONE BY:

J.M. Blair

J.M. Hush

E.C. Kleme

L.W. Seagondollar

R.F. Taschek

C.M. Turner

REPORT WRITTEN BY:

Part I - R.F. Taschek

Part II - C.M. Turner

UNCLASSIFIED

[redacted]

ABSTRACT

The 25 fission cross section ratios σ 30 Kev/σ 1 Mev, σ 250 Kev/σ 1 Mev and σ 600 Kev / σ 1 Mev have been determined by use of the Be^7 activity in a Li target bombarded with protons. These measurements show that the cross section at 30 Kev is about 30% lower than the value found in the old long-counter measurements (LA-150). Absolute values of σ 250 Kev, σ 600 Kev and σ 1 Mev have been determined by Mn bath measurements of the flux from the Li (pn) reaction and verify the values found by the Be^7-activity method.

FISSION CROSS SECTIONS BY THE Be^7 AND [redacted] METHODS

PART I - FISSION CROSS SECTION RATIOS BY THE Be^7 METHOD

INTRODUCTION

Long-counter[1] extrapolation of the 25 fission cross section from 1 Mev to low energies combined with measurements[2) $\sigma_a(B)/\sigma_f(25)$ and $\sigma_a Li/\sigma_f(25)$ makes the shapes of the $\sigma_a(B)$ resonance at 100 Kev and the $\sigma_a(Li)$ resonance at 260 Kev difficult to understand theoretically and thus throws doubt on the low-energy fission cross section. For this reason special emphasis has been placed on measuring the ratio $\sigma_f(29\ Kev)/\sigma_f(1\ Mev)$ accurately and independently of the long counter. The method used in this experiment was to monitor the total flux of neutrons from the Li^7 $(p,n)Be^7$ reaction by the 41-day γ activity of the Be^7. The reaction goes as follows:

$$Li^7 + p \rightarrow n + Be^7;$$

$$Be^7 \xrightarrow{41d} Li^7 + e^k \text{ about 90\% of the time}$$

$$Be^7 \xrightarrow{41d} Li^{7*} + e^k \text{ about 10\% of the time}$$

$$Li^{7*} \rightarrow Li^7 + h\nu;\ 480\ Kev\ \gamma ray$$

Thus if the branching ratio at Be^7 remains independent of the proton energy, the γ activity of the Li target determines the total number of neutrons emitted during a given bombardment. It should be possible to make an absolute determination of the branching ratio and number of γ's, and thus the total neutron yield, by counting γ ray and k capture x-ray coincidences. Another way to find the absolute neutron yield would be to make a spectrochemical analysis for

---

1) LA-150
2) Ibid.

[redacted]

the 41-day Be^7 produced in a thick Li target given a long proton bombardment. One can estimate that a target of about 6 mg/cm^2 (thick for 2.3-Mev protons) Li bombarded at 30 μa on the short electrostatic generator for 10 hours with 2.3-Mev protons would give about 3 x 10^{-8} gm Be^7, which should be rather accurately ($\lesssim$5%) measurable, especially since the γ activity allows a partial chemical separation to be made with good knowledge of the fraction of Be^7 left in the extracted sample. The γ ray activity in standard conditions combined with the chemical Be^7 determination would give the γ's/neutron and this number would then apply to all thicknesses of target, since thin targets are used for fission measurements. Using the γ activity/neutron the complete total-yield curve for the Li (p,n) reaction could be determined absolutely.

Since Koontz's[3] measurements had accurately determined the absolute 25 fission cross section at 1 Mev it was decided that the most immediately useful measurements would be cross section ratios at several different energies to the 1-Mev value using the Be^7 activity as a monitor only.

METHOD

The experimental procedure was as follows: For a given Li target the fissions in a 25 foil per μcoulomb of protons were determined for forward neutrons of some energy; the net γ-ray activity for this particular bombardment then gave either the γ's/fission or γ's/μcoul. Since the γ-ray activity is proportional to the <u>total</u> neutron flux it was then necessary to make an angular distribution measurement, during which the γ's/μcoul were frequently determined to make sure there was no deterioration or other change in the target. From the angular distribution the fraction β of all neutrons going through the fission foil in the

3) LA-128

forward direction was found. The same procedure at 1 Mev then gives

$$\frac{\sigma_f(E_n)}{\sigma_f(1\ \text{Mev})} = \left(\frac{F}{\gamma}\right)_{E_n} \Big/ \left(\frac{F}{\gamma}\right)_{1\ \text{Mev}} \cdot \frac{\beta_{1\ \text{Mev}}}{\beta_{E_n}}$$

where $(F/\gamma)_{E_n}$ are the fissions/activity at the energy E_n and β_{E_n} is the fraction of all the neutrons going through the foil, as found from the angular distribution.

Special emphasis was placed on determining $\sigma_f(29\ \text{Kev})/\sigma_f(1\ \text{Mev})$ since at low energy the most deviation from the long-counter data was expected. A 29-Kev measurement was especially adaptable to this method because the momentum relations in the Li(p,n) reaction just at threshold cause the neutrons to come out in a very narrow cone in the forward direction; if now either the energy is controlled well enough to keep a fission foil exactly in the whole cone, or if a very uniform foil is used and the cone always confined inside its area, then no angular distribution measurements need be made, since <u>all</u> the neutrons pass either through the whole foil, or all pass through a portion of it which is of known thickness. The second method was followed since it is much easier to prepare a uniform fission foil than to hold the proton energy constant to the degree required.

Fig. 1 shows the two methods used to measure the γ activity. A thin-walled Geiger counter of the Chicago type was mounted in a 1-inch-thick cylindrical lead shield and suspended from a trolley so it could be rolled on and off the target tube, which entered the Pb shield through a 1-3/4-inch hole. Two standard counting positions were used depending on whether the large rotating or small, fixed Mn-bath target was in place. The γ intensity after passing through 10 mils of target backing material (tantalum) was large in most cases but several runs could be made on a single target before the activity was so large that

[redacted]

entirely fresh Li had to be evaporated. In those cases where low activities were expected, as in all the 29-Kev data, even the Ta backing was replaced for each run since for these thin Li targets the Be^7 center of gravity energy is sufficient to cause it to stick to the Ta.

The following checks were made to assure that other reactions were not confusing the Be^7 activity measurements:

1) the tantalum backing was bombarded at several energies above and below the Li(p,n) threshold;

2) a Li target on Ta was bombarded with protons of energy just below the Li(p,n) threshold;

3) blocks of metallic Li and Ta were given strong neutron irradiations at several energies including thermals;

in none of these experiments were any activities observed of appreciable intensity. It was, however, found that for those irradiations made in the Mn bath (see below) several inches of the target tube also had to be made of tantalum since the iron and aluminum previously used became appreciably active in these strong slow-neutron fluxes. The activity of a strongly exposed target was followed for about 80 days and no long-period activity other than the 41-day was observed.

The observations made at neutron energies other than 29 Kev were as follows: The fissions from thin and uniformly deposited 25 foils were observed in the forward direction, a half angle of 11° being subtended at the target by foil RFT1 and $11^\circ 35'$ by foil PXP34A4. The net γ activity was measured immediately after the exposure, several on-off readings being taken to assure accurate placement of the target, checks on short-lived activities, and on background; all readings were standardized to a uranium-glass count. For the angular distribution,

[redacted]

fissions/μcoul with the same or other foils were determined at various angles on both sides of the target, the net activity per μcoul being observed several times; direct proportionality between γactivity and proton current showed that there was no appreciable change in the target while the measurements were made. The angular distributions as observed had to be corrected at large angles for the change in 25 cross section. This correction is very small for the 1 Mev data but appreciable for the lowest energies and will be discussed in detail below.

For the 29-Kev data, the proton energy was set very close to the Li(p,n) threshold and the fission chamber put as close to the target as possible, about 1/4 inch; small fluctuations in proton energy would then cause bursts of neutrons to pass through the fission foil, but the fluctuations were never allowed to become large enough for the neutron cone to go outside the foil. This latter effect was checked on the long electrostatic generator, where the energy control is least steady, by putting the fission chamber at about 45° from the center line; no appreciable number of fissions were observed. Long exposures were necessary at this energy because the total number of neutrons, and therefore the γ activities are small compared to the high-energy data.

The first measurements of σ_f(29 Kev)/σ_f(1 Mev) gave a value for the 29-Kev cross section about 25% lower than the long-counter extrapolation; it was decided to make Mn-bath comparisons with Be^7 activity for the same exposures to be sure no unknown effect was causing the difference. The Mn-bath method of determining neutron fluxes is essentially identical to the Be^7 and in addition the bath can be calibrated by a known neutron source. The threshold tickling method of determining σ_f(29), however, is not applicable to the bath since there is no method of measuring fissions, the bath surrounding the target during exposure.

Ratios of Be^7 to Mn activities were determined for 29-Kev, 250-Kev, 600-Kev, and 1-Mev neutrons in the forward direction; these ratios were constant within the limits of error in the experiment and showed that both methods measured the same quantity, i.e., total number of neutrons emitted.

RESULTS

Table I shows the ratio of Be^7 activity to Mn-bath activity for the same exposure at a number of different energies. It will be seen that there is ~6% mean deviation in all the ratios; this, however, arises mainly from a group of measurements which showed a definite drift in time, independent of energy; thus the 1-Mev data on target 8 gives a larger ratio than that on target 2 indicating that the 250-Kev data of target 6 is also high. The 6% mean error is not normalized to the drift indicated. The Be^7 activities could not be accurately determined since only short exposures could be made with the Mn bath on the target; when successive exposures were made on the same target the previous activity became background for the following one also increasing counting error. The error of 6.4% is within the statistical counting error of my individual exposure.

At this time comparisons were also made of the target activity per μcoulomb of protons with Mn bath on (i.e. in slow-neutron flux) to bath off at forward neutron energies of 250, 600 and 1000 Kev. It was found that the average of all runs (about 10) gave a 6% higher activity per μcoul for bath on than bath off; this was assumed to be the long-lived activity in Ta and since it was so small for a very large slow flux it was not considered at all important in the usual procedure of finding the activity, i.e., with no slowing-down material present at all.

Table II shows the results for five separate runs to determine $\sigma_{29\ Kev}/\sigma_{1\ Mev}$. The conditions, which were widely different in many cases, are listed. Using 1.33 barns for the 1 Mev cross section, $\sigma_{29.1\ Kev} = 2.30$ 3%

where the error indicated is the mean deviation in the 5 runs. The probable error may be around 5% since the measurements also involve the 1-Mev angular distribution. These data were taken carefully with respect to getting good counting statistics on the small 29-Kev activity. Fig. 2 shows the growth of activity with exposure for both 29 Kev and 1 Mev in Run No. 1.

The cross section of 2.30 barns is only 71% of the LA-150 value of 3.24 barns; this latter value has a probable error of approximately 10%.

In order to obtain the 29-Kev cross section the 1-Mev angular distribution must be known, as outlined above. In Table III are shown the angular distribution data taken with a fission foil which subtended a half angle of $11^{\circ}35'$ at the target. The observations consist of fissions per microcoulomb of protons at the angles listed; at each angle the neutron energy is given and goes down to 345 Kev at 180°. The 180°-values are from an extrapolation of the data in circular coordinates, which is quite good. For each of these energies the cross section according to LA-150 is used to determine $\left(\frac{F/\mu c}{\sigma}\right) = Y$, the true angular distribution. The change in cross section with energy is small in this energy region and probably quite accurately known; in any case the yield at large angles is affected most and here the number of neutrons is only a small fraction of the total. In Column seven are listed some early data taken at a closer distance and normalized to those in column six at zero degrees. It has been found[4] that the angular distribution from the Li(p,n) reaction can be fairly well represented by

$$Y'(\Theta',E) = A + B\cos\Theta' + C\cos^2\Theta'$$

where Y' is the yield in the center of gravity system and Θ' the center of gravity

4) CF-638

system and θ' the center of gravity angle, A, B, and C are functions of the proton energy. In column eight are listed the values of Y in the laboratory system obtained by determining A, B and C from the center of gravity angles 0°, 60° and 150°; the fit to the observations is quite good. By integrating Y' sin θ' over the angle subtended by the detector one finds the fraction of all neutrons passing through the foil at 0°, since the total yield on this basis is $2A+(2/3)C$. This fraction is given in the table together with the fraction determined by a planimeter integration of Y sin θ from the actual observations. In all cases the planimeter integrations were used to determine the cross section ratios. Fig. 3 shows the angular distribution Y and Y sin θ for E_n(ave)= 1000 Kev at 0°.

Tables IV and V, respectively, list the angular distribution data for 600 Kev and 250 Kev forward neutron energy, similarly to that for 1 Mev. In the 600-Kev data it will be seen that in addition to a correction using the LA-150 fission cross section, an assumed cross section is also used; this latter σ_1 begins to fall appreciably below σ_{LA150} at about 380 Kev chosen since this is about the minimum neutron energy for E_n = 1000 Kev forward. Since, however, the minimum neutron energy is still 160 Kev at 180° in this case the total yield and therefore the fraction in the forward direction is not appreciably affected. Thus 2.77% go into the 11° half angle assuming LA-150 and 2.70% assuming σ_1. The fit obtained from $Y= 1.021 + 0.796 \cos\theta' + 0.1125 \cos^2\theta'$ is quite good and gives 2.81% in 11° half angle. Different fission foils were used in these data. To compare angular distributions multiply the 1-Mev yields by 8.65 and therefore also A, B and C.

Table V contains still a third cross section σ_2, assumed for correcting the observations with the fission detector. σ_2 begins to deviate from σ_{LA150} at about 160 Kev chosen since this is the minimum energy for

E_n(ave)= 600 Kev forward, and passes through the Be^7 cross section earlier obtained for 29.1 Kev. The fit from $Y' = 0.3179 - 0.0684 \cos\theta' - 0.0205 \cos^2\theta'$ is not very good, but gives 1.62% in the 11^o half angle using the σ_1 correction. Planimeter integration gives 1.90% assuming σ_{LA150}, 1.68% assuming σ_1 and 1.64% assuming σ_2. Figs. 4 and 5 show Y and Y sin θ for 600 Kev and 250 Kev for those values of σ.

Table VI lists the 600-Kev and 250-Kev fission and activity data; these data were not determined with the accuracy of the 29.1- and 1000-Kev data since the 29.1-Kev cross section obtained by the Be^7 method already indicated that there would be an ambiguity in the angular distribution determinations, especially at 250 Kev where the backward neutrons have an energy as low as 23 Kev.

In Table VII are given the values of the cross section as determined from the ratio to 1000 Kev and the fraction β of neutrons falling into the 11^o half angle according to the various assumptions as to the variation of σ with angle. At 600 Kev either choice of cross section variation gives about the same σ_{calc} with perhaps a slightly better fit if σ of LA-150 clear down to 23 Kev is much the worst of the three, deviating by more than 20% from the 250-Kev value given in LA-150. The choice of σ_1 or σ_2 give approximately the same answer, with σ_2 perhaps slightly better. Although these data do not at all serve to determine the 250-Kev fission cross section accurately, they indicate that an assumed cross section falling below σ of LA-150 from about 160 Kev on and passing through the Be^7 value of 2.30 barns at 29.4 Kev gives a much better value at 250 Kev than the σ of LA-150 curve. Thus the 250-Kev data here obtained serves mainly to corroborate the 29.1-Kev data without establishing the trend of the fission cross section closely. Unfortunately, only the shape and not the absolute value of cross section is important in the angular distribution. Fig. 6 shows σ of LA-150

and the two assumed cross sections σ_1 and σ_2. On the same plot are shown the values of the fission cross section obtained in this experiment. The 29.1-Kev value is shown with the mean deviation of 5 different runs. The 250-Kev data have a mean deviation of 5% in F/γ from 3 short runs, and the 600-Kev data, 2.5% in F/γ from two runs; however, because of the ambiguity in angular distribution and the fairly large statistical error in counting the target activity these points are plotted with a 10% error.

It is believed that the value of $\bar{\sigma}_{29.1}/\bar{\sigma}_{1000}$ and thus $\bar{\sigma}_{29.1\ Kev}$ here determined is quite good and the expected error much smaller than the difference between the Be^7 value of $\bar{\sigma}_{29}$ and the La-150 value. There are three effects, which if important, would make the observed fission count at 29 Kev too high and thus make the determined $\bar{\sigma}_{29.1}$ even too high; these effects are, 1) the extreme obliquity of some of the neutrons striking the foil when the foil is about 1/4" from the target; 2) the presence of a very slow group of neutrons slightly above the Li(p,n) threshold; and 3) the presence of a slow-neutron room background. In addition, any loss of target material would decrease the activity and thus also give too high a value to F/γ; this was checked several times in any one run by plotting activity against proton current and found linear in all but one case. The one effect at 29.1 Kev which could make the cross section seriously low is that in the threshold "tickel" the energy fluctuations above threshold could be large enough to throw the edges of the neutron cone outside of the fission foil; this was checked by placing a detector at 45° to the target and operating as in taking the 29-Kev data. It was found that under usual operating conditions very few neutrons got outside of 45° and this was not considered important since the foil usually subtended a half angle of about 60°.

Recent measurements[5] with a long counter adjusted for deviations from

5) Bailey - in progress.

flatness indicate that $\sigma_{29\ Kev}$ given above is essentially correct and that the energy dependence of σ lies somewhere between σ_1 to σ_2 in Fig. 6. Experiments[6] using an Sb-Be source also indicate that the low value at 30 Kev is correct.

The effective energy of the neutrons in a threshold tickle should actually be between 30 and 35 Kev for a 1/v detector depending on how high above threshold the energy fluctuations go but σ obtained here has been plotted at 30 Kev.

---

6) Seagondollar and Hanson - Monthly Report of R Division, September, 1945.

TABLE I.

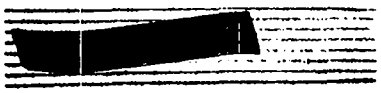

Target	E_n (0^o)	Be^7 Activity (counts/20 min)	Mn-bath Activity (counts/min)	Be^7 Activity / Mn Activity
2	29 Kev	241	34.98	6.91
2	1 Mev	590	82.7	7.14
3	30 Kev	262	37.0 (counter banged)	7.09
3	1 Mev	257	34.6	7.46
4	250 Kev	50.4	5.97	8.44
6	250 Kev	228	26.7	8.55
6	250 Kev	296	36.7	8.07
8	1000 Kev	264	33.3	7.94
8	1000 Kev	250	32.4	7.74
9	600 Kev	341	47.4	7.19
			Simple Ave =	7.65 ± 6.4%

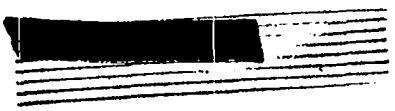

TABLE II.

Run No.	Foil	Condition	E_n	Fissions	Net Activity	Fissions/γ	$\frac{(F/\gamma)_{29\ Kev}}{(F/\delta)_{1\ Mev}}$	$\frac{\bar{\sigma}_{29\ Kev}}{\bar{\sigma}_{1\ Mev}}$	$\bar{\sigma}_{29\ Kev}$	
1	PXP34A4 2.77% of neuts pass through at 1 Mev	Long Tank 1-5/8" Target counted at inside edge of Pb shield. Good runs.	30 Kev	25,664	83.35	313				
			1 Mev	6,009	0.0547	5.07_3	61.8	1.691	2.25	.05
				0.2778 fs/μcoul from curve	γs/μcoul from curve					
2	"	"	30 Kev	36,752	152.3	240				
		Poor 29 Kev run, lost some of target	1 Mev	2,020	572	3.54	68.1	1.88	2.51	.21
3	"	Short Tank 29 Kev	30 Kev	47,424	189.2	251				
		Long Tank 1 Mev 1-5/8" target Good runs		3,776	880.3	4.29	58.7	1.62	2.16	.14
4	RFT 1 2.50% of neuts pass through at 1 Mev	Long Tank, 1 cm target counted at 1/8" from Geiger counter	30 Kev	74,130	125.5	591				
			1 Mev	7,865	934	8.43	70.2	1.75_5	2.34	.04
5	"	"	30 Kev	90,824	156.5	579				
			1 Mev	9,883	1187	8.33	69.6	1.74	2.32	.02

Average = 2.30 ± .07 from weighted average by number of 29-Kev fissions.

$\bar{\sigma}_{29.4\ Kev}$ (LA-150) = 3.24 barns

APPROVED FOR PUBLIC RELEASE

APPROVED FOR PUBLIC RELEASE

TABLE III

Angular Distribution for $E_p = 2.670$ Mev, forward neutron energy 1.0 Mev, target thickness 40 Kev.
Data taken with fission foil PXP34A4 at 3" subtending $11^\circ 35'$ half angle at target.
σ from LA-150 used to correct high-angle yields.

θ_{Lab}	θ_{cg}	E_n(Kev)	$(F/\mu c)_{ave}$	σ_{LA150}	$\left(\frac{F/\mu c}{\sigma}\right)_{3"} = Y$	$\left(\frac{F/\mu c}{\sigma}\right)_{2\frac{13}{32}"}$	$\left(\frac{F/\mu c}{\sigma}\right)_{calc} =$
0°	0°	1000	0.2778 ± 0.0035	1 33	C.2082	0.2082	[0.2082]
12°		990	0.2727 ± 0.045	1.33	0.2047	-	
$22\text{-}1/2^\circ$		960	0.2557 ± 0.045	1.33	0.1920	0.188	
45°		810	0.186 ± 0.005	1.34	0.1387	0.131	
$67\text{-}1/2^\circ$		725	0.1192 ± 0.003	1.36	0.0879	0.0891	
90°		590	0.0726 ± 0.005	1.39	0.0522	0.0502	
135°		405	0.0398 ± 0.002	1.48	0.0268	-	
(180° extrapolated from polar plot)		345	(0.032)	(1.57)	(0.0213)	-	0.0207

Data of the following angles were taken from a curve of the above to make a convenient fit with $Y' = A + B\cos\theta' + C\cos^2\theta'$
The observations at $\theta_{cg} = 0^\circ, 60^\circ$ and 120° were used to determine A, B, and C; and are in brackets.

24°	30°		0.1895	0.1904
49°	60°		0.1290	[0.1290]
$75\text{-}1/2^\circ$	90°		0.0733	0.0718
$105\text{-}1/2^\circ$	120°		0.0391	[0.0391]
$140\text{-}1/2^\circ$	150°		0.0257	0.0253

This fit gives $Y(\theta') = 0.06512 + 0.0489\cos\theta' + 0.02345\cos^2\theta'$; $\int_0^{13^\circ 49'} Y' \sin\theta' d\theta' / 2A + 2/3C = 2.70\%$

Planimeter Integration gives 2.50%

TABLE IV

Angular Distribution for E_p(max)= 2.330, E_n (max)= 625 Kev, E_n(ave)= 605 Kev for 40-Kev target.
Data taken with fission foils E9B and E5C, 3" from target.

θ_{lab}	θ'_{cg}	E_n(Kev)	$(F/\mu c)_{ave}$	σ_{LA150}	σ_1 assumed below 380 Kev	$\left(\frac{F/\mu c}{\sigma_{LA150}}\right)$	$\left(\frac{F/\mu c}{\sigma_{assm}}\right)$	$\left(\frac{F/\mu c}{\sigma_{assm}}\right)_{calc} = Y$
0°	0°	605 ± 7	4.38 ± 0.18	1.40	1.40	3.124	3.124	3.385
23°	30°	570 ± 15	4.33 ± 0.02	1.40	1.41	3.09	3.07	[3.070]
47°	60°	492 ± 20	3.10 ± 0.04	1.41	1.42	2.20	2.18	2.015
72-1/2°	90°	383 ± 40	1.74 ± 0.07	1.52	1.48	1.143	1.174	[1.174]
102°	120°	268 ± 32	0.837 ± 0.017	1.70	1.52	0.492	0.551	0.534
138°	150°	188 ± 16	0.372 ± 0.0	1.90	1.61	0.196	0.231	[0.231]
180° from polar plot	180°	(160 ± 3)	(0.310)	2.00	1.66	0.155	0.1868	0.155

The fit to the above data at θ'=30°, 90° and 150° gives

$$Y' = 1.021 + 0.796 \cos\theta' + 0.1125 \cos^2\theta' \text{ from which } \frac{\int_0^{14.5^\circ} Y' \sin\theta' \, d\theta'}{2A\left(\frac{2}{3}C\right)} = 0.0281$$

or 2.81% in 11° half angle for the assumed σ_1

Planimeter integration of distribution gives

2.70% in 11° for assumed cross section,

and 2.77% in 11° for LA150 cross section.

APPROVED FOR PUBLIC RELEASE

TABLE V

Angular Distribution for $E_p(max) = 2.002$ Mev, $E_n(max) = 259$ Kev, $E_n(ave) = 249$ Kev for 23-Kev target.
Data taken both with fission foils E9B and E5C and with PXP34A4 at 3" from target.

θ_{lab}	θ°_{cg}	E_n(Kev)	$(F/\mu c)_{ave}$	σ_{LA150}	$F/\sigma\mu c$	σ_1	$\left(\frac{F/\mu c}{\sigma_1}\right)$	σ_2	$\left(\frac{F/\mu c}{\sigma_2}\right)$	$\left(\frac{F/\mu c}{\sigma_1}\right)$ calc
0°	0°	249 ± 5	0.839 ± 0.011	1.72	0.488	1.53	0.548	1.72	0.488	[0.548]
$19\text{-}1/2^\circ$	30°	235 ± 13	0.861 ± 0.011	1.77	0.487	1.54	0.559	1.77	0.487	0.551
40°	60°	192 ± 22	0.845 ± 0.014	1.89	0.447	1.60	0.528	1.89	0.447	0.538
$61\text{-}1/2^\circ$	90°	135 ± 23	0.791 ± 0.014	2.09	0.378	1.69	0.468	2.02	0.391	[0.468]
87°	120°	77 ± 15	0.521 ± 0.011	2.58	0.202	1.89	0.275	2.15	0.242	0.312
123°	150°	37 ± 6	0.301 ± 0.005	3.03	0.0994	2.24	0.1343	2.26	0.133	[0.134]
180°	180°	22.5	0.21	3.42	0.0614	2.50	0.0841	2.34	0.0899	0.0861

from polar plot

The fit to $\frac{F/\mu c}{\sigma_1}$ at $\theta^\circ = 0^\circ$, 90° and 150° gives

$$Y^\circ = 0.3179 - 0.0684 \cos\theta^\circ - 0.0205 \cos^2\theta^\circ$$ from which $$\frac{\int_0^{16^\circ 55^\circ} Y^\circ \sin\theta^\circ \, d\theta^\circ}{2A + \frac{2}{3}C} = 1.62\%$$ in 11° half angle.

Planimeter integration gives following

1.90% assuming σ_{LA150}

1.68% assuming σ_1

1.64% assuming σ_2

APPROVED FOR PUBLIC RELEASE

[redacted]

TABLE VI

Fission and Activity Data

Run #	Activity = γ counts/20 min	Fissions	F/γ	(F/γ) ave
600-Kev neutrons forward				
1	381	4200	11.00	10.70 ± 2.5%
2	520	5450	10.48	
250-Kev neutrons forward				
1	358	2378	6.63	6.35 ± 4.7%
2	370	2410	6.52	
3	778	4590	5.90	
1000-Kev several runs			8.38	8.38

$$\sigma_{E_n} = \frac{(F/\gamma)_{E_n}}{(F/\gamma)_{1000\ Kev}} \times \frac{\beta_{1000\ Kev}}{\beta_{E_n}} \times 1.33 \text{ barns}$$

[redacted]

TABLE VII

E_n(Kev)	$\left(\frac{F}{\gamma}\right)_{ave}$	σ used to correct angular distribution	β	σ_{LA150}	σ_{calc}	$\frac{\sigma_{calc}}{\sigma_{LA150}}$
1000	8.38	σ_{LA150}	2.50%	1.33	-	
600	10.70	σ_{LA150}	2.77%	1.39	1.53	1.10
		σ_1	2.70%		1.57	1.13
250	6.35	σ_{LA150}	1.90%		1.33	0.774
		σ_1	1.68%	1.72	1.50	0.874
		σ_2	1.64%		1.54	0.895

APPROVED FOR PUBLIC RELEASE

FIG. 1

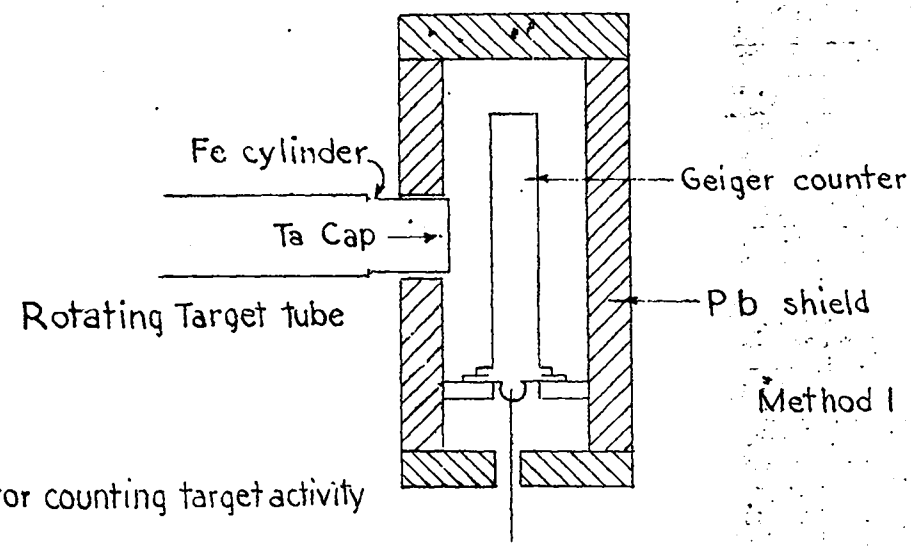

Methods used for counting target activity

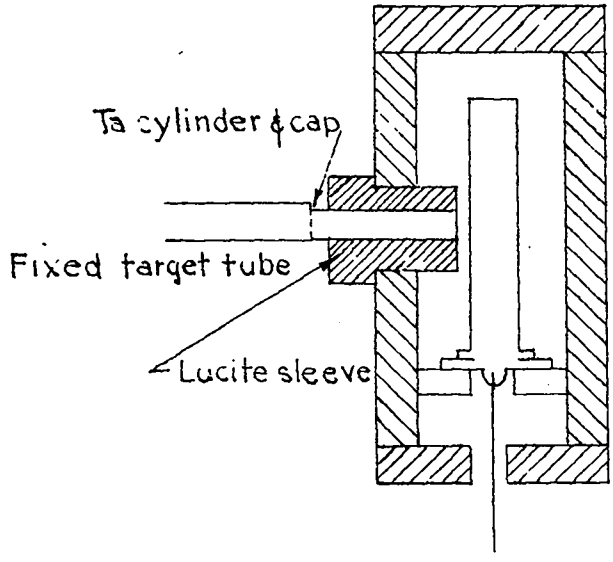

Method for confining total neutron flux of 29-Kev energy to fission foil

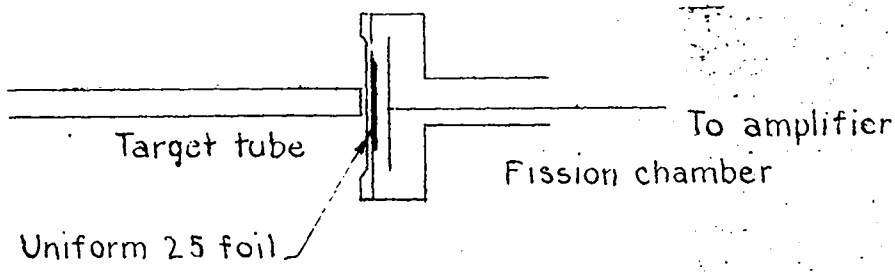

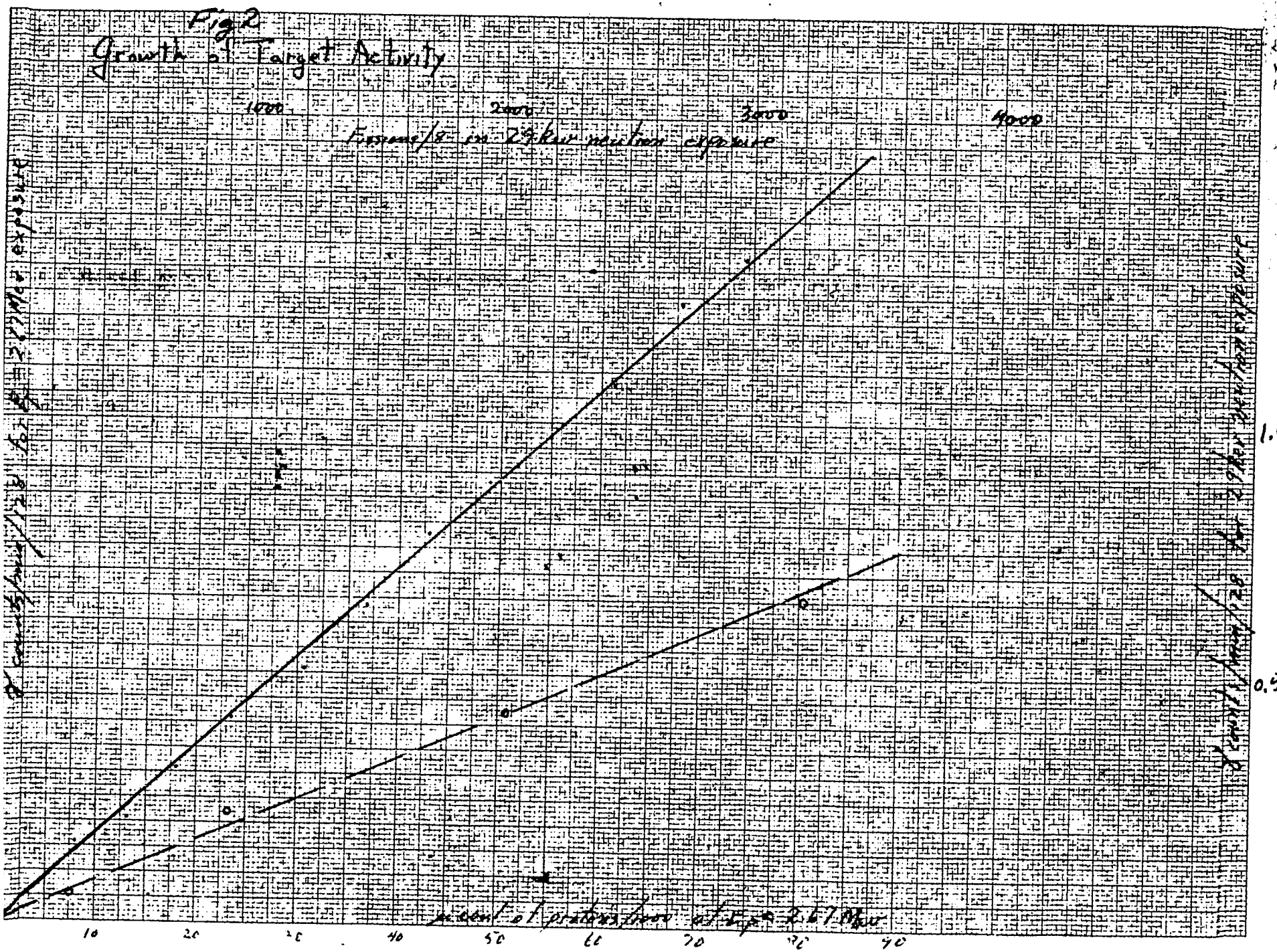

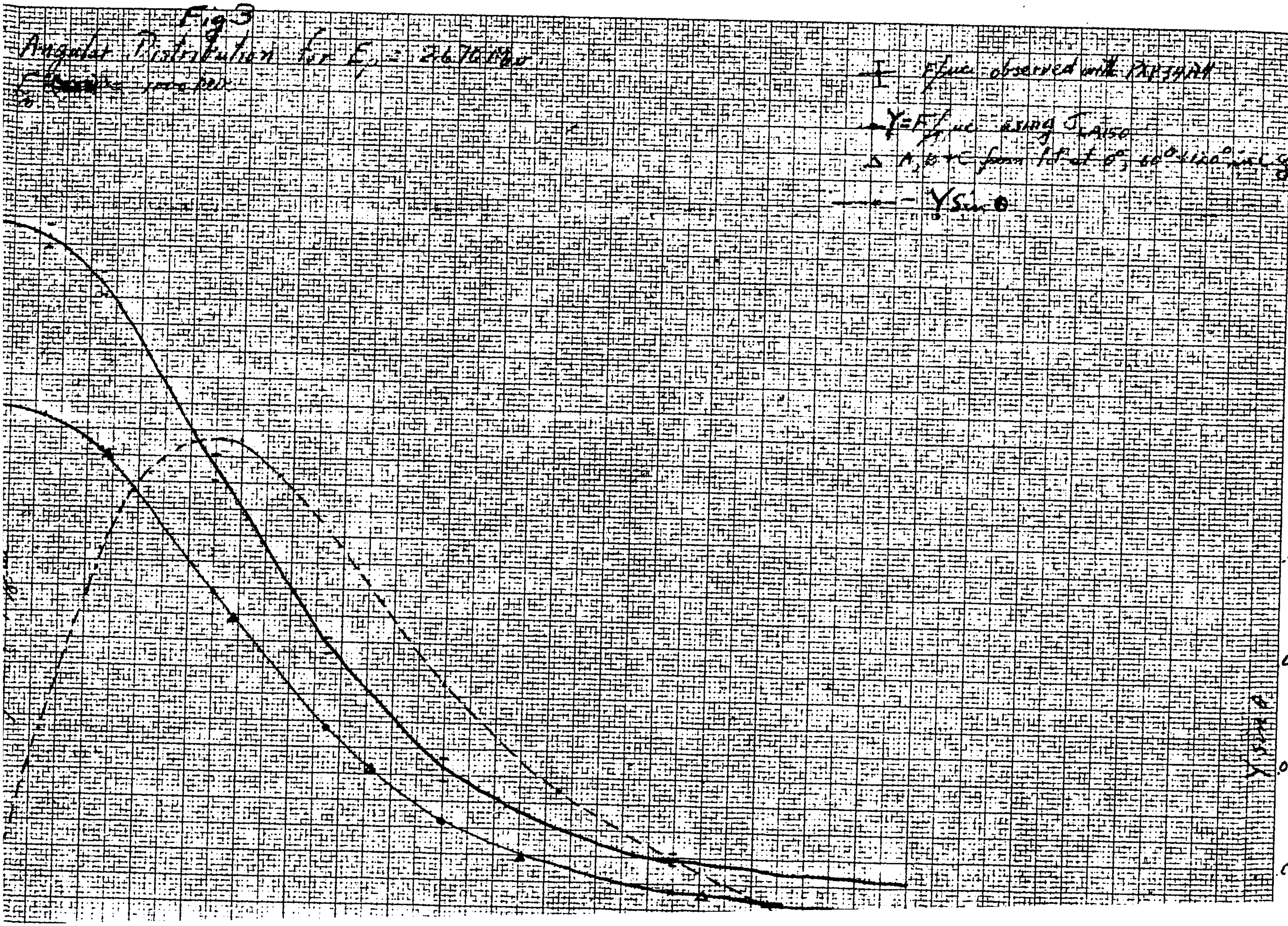

APPROVED FOR PUBLIC RELEASE

Fig 4

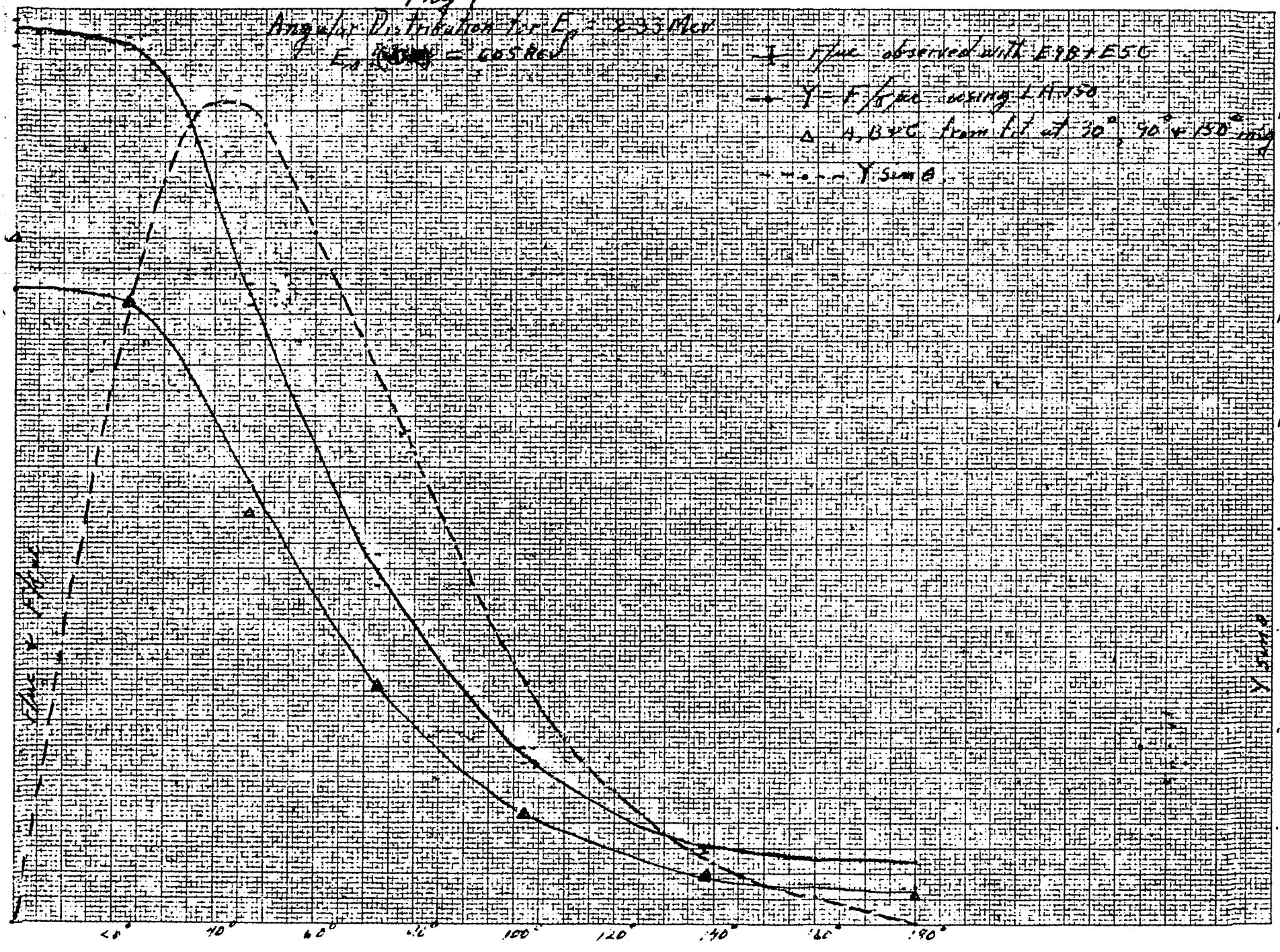

APPROVED FOR PUBLIC RELEASE

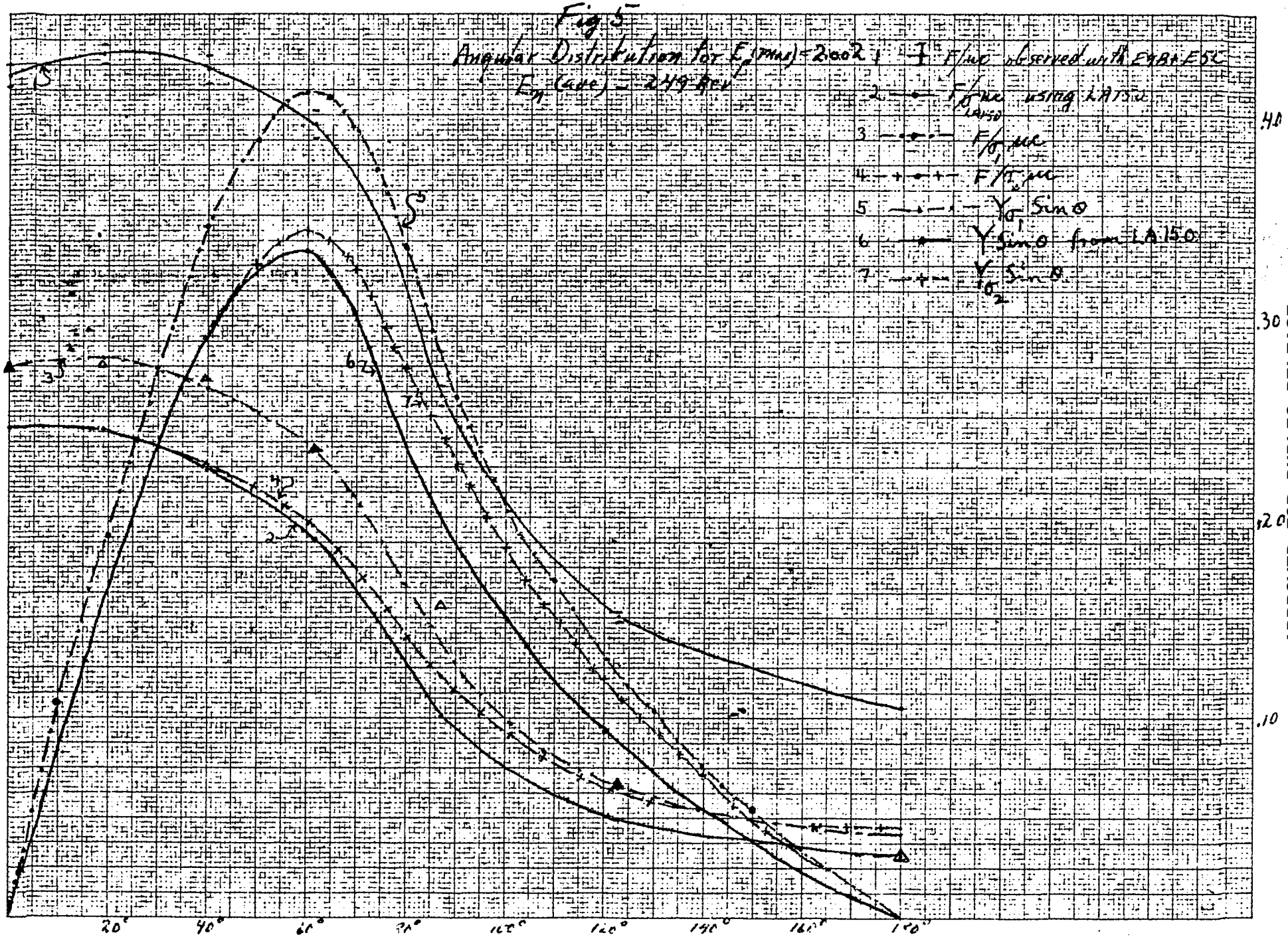

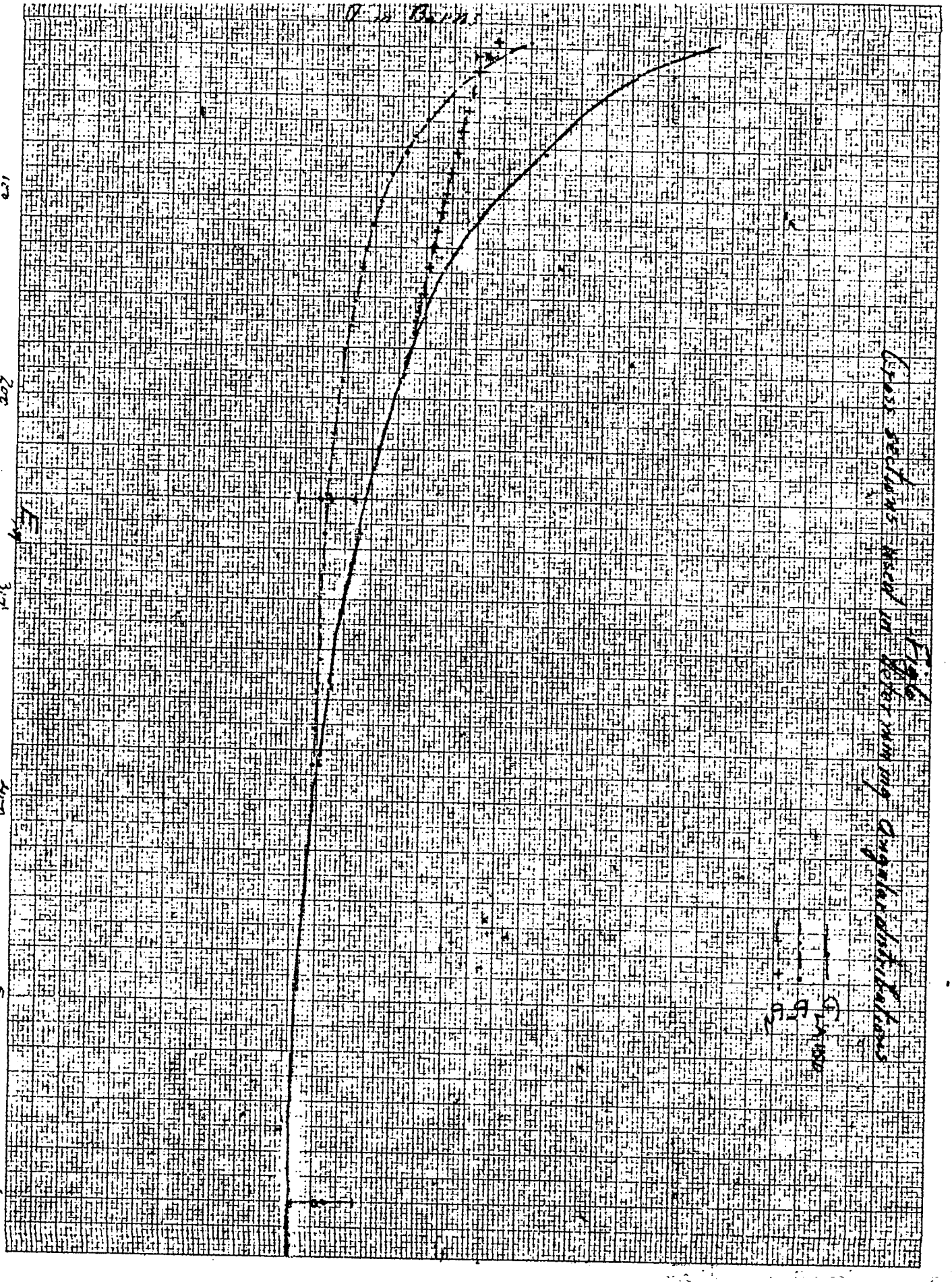

[redacted]

PART II - FISSION CROSS SECTIONS BY THE MANGANESE-BATH METHOD

I. INTRODUCTION

A measurement of the 25 fission cross section by Benedict and Hanson[7] using the manganese bath method for determining the neutron flux gave values somewhat lower than those obtained using the coincidence proportional counter method. Since other measurements made subsequently tended to fall in between these values, it was decided to repeat the measurement with the manganese bath in order to get as many checks as possible, particularly on the 1-Mev cross section.

II. THE MANGANESE-BATH TECHNIQUE

The manganese bath provides a method for comparing neutron source strengths. The neutron source in question is placed at the center of a tank containing a water solution of a manganese salt, - usually $MnSO_4$. The neutrons emitted by the source are slowed down by the hydrogen in the water and are captured in part by the manganese, the reaction being,

$$Mn^{55} + \gamma \rightarrow Mn^{56}. \qquad (1)$$

Since manganese consists entirely of the isotope 55 there are no competing reactions to confuse matters. The Mn^{56} is radioactive and decays with a half-life of 2.59 hours, emitting both beta and gamma rays. For a given irradiation time and solution concentration the number of activated atoms, as determined by Geiger counting in a standard geometry, is proportional to the neutron source strength.

The technique of counting the activated manganese usually used heretofore consisted of precipitating the manganese out of a sample of the solution as MnO_2, drying, and packing in a standard geometry around a thin-wall Geiger counter. This method had the advantage that it concentrated the manganese, but it had the following

[redacted]

7) CF-638

disadvantages which made it impractical for use in a long series of runs: (1) it was extremely messy and time-consuming; it took about 4 hours to perform the precipitation and drying procedures and during this time the activity decreased; (2) it required the addition of $MnSO_4$ after each run to replace that precipitated out; this required accurate weighing of $MnSO_4$ with known water of hydration in order to avoid changing the manganese concentration in the solution.

In view of these disadvantages it was decided to try immersing the Geiger counter directly in a sample of the irradiated solution. Preliminary estimates indicated that a sufficient counting rate could be obtained in this manner and later experience showed it to be quite adequate for the experiments in which we were interested. Using a 1-gram radium-beryllium source (8.88×10^6 neutrons/sec) with a 12-hour exposure, and with a manganese concentration of about 200 grams of $MnSO_4 \cdot 4H_2O$ per liter, the counting rate was 32.1 scale-of-64 counts/minute. Fig. 7 shows the Geiger-counter arrangement used. "A" is a standard lead counter shield turned up on end so the counter "B" points downward. "C" is a lucite container for the manganese solution samples to be counted. This was filled to a standard height so that when the counter was immersed the liquid covered the sensitive portion of the counter. In this way the counting geometry was accurately reproducible. This system proved to be so much more convenient and reliable than the old precipitation method that it became practical to make numerous runs. Reproducibility of around 1% to 2% was easily obtained on Ra-Be source runs.

Tank

Fig. 8 shows the dimensions of the tank used to contain the manganese solution. In determining tank size a compromise has to be made between neutron leakage and counting rate. The larger the tank the fewer will be the neutrons which get out without being captured, but the activated manganese will be distributed through

[redacted]

a larger volume so the resulting Geiger counting rate will be lower.

For a tank of this size the leakage of Ra-Be neutrons has been calculated to be 4.3% (CF-638). The leakage of Li(p,n) neutrons has been assumed to be zero, since the primary energy is so much lower than the Ra-Be neutron energy. The leakage of Ra-Be neutrons will cause the value obtained for the cross section to be too low (see equations 16 and 18 of appendix) so the computed values must be increased by 4.3%.

Stirring

After each irradiation, the solution has to be thoroughly stirred to distribute the activity uniformly throughout the volume. It was found that about 5 minutes stirring with a hand stirrer consisting of a 6" diameter disc fastened on the end of a rod was adequate.

Sampling

Before each irradiation of the bath a sample was removed to give the background due to previous irradiations and pickup from the electrostatic generators. This sample was saved and counted just after the active sample. After counting, the samples were returned to the tank so the volume and concentration of the solution remains constant.

Use of SO_2

At the suggestion of Segre, the solution was saturated with SO_2 to reduce the likelihood of a preferential precipitation of the activated manganese from the solution. Consistent results were obtained without the SO_2, however, so it was probably unnecessary.

[redacted]

Mn Concentration [redacted]

The approximate concentration of manganese used was 200 grams of $MnSo_4 \cdot 4H_2O$ per liter, which is approximately 1/5 the saturation value of room temperature. A rough calculation shows that with this concentration about 50% of the neutrons are captured by manganese.

Lithium Target

Fig. 9 shows the lithium target assembly used to produce the neutrons. The tubes were made of dural to avoid slow-neutron absorbing materials. As indicated, an electron barrier arrangement was used to prevent secondary electrons from either entering or leaving the cup containing the lithium target. This was necessary in order that an accurate measure of the quantity of proton charge striking the target be obtained since this was used as an intermediate monitor between runs in which the bath was activated and runs in which fissions were counted. Care was taken to limit the proton beam to a value such that the target did not get hot enough to evaporate the lithium. It was found that if the current was limited to about 2 microamperes no appreciable change of neutron yield occurred during our runs.

The lithium target was evaporated in an auxiliary system, transferred to the long tank target tube in an atmosphere of argon, and then evacuated quickly so that no appreciable oxidation could occur.

MEASUREMENT OF THE 25 FISSION CROSS SECTION

The method of measuring the 25 fission cross section with the manganese bath was as follows: (1) the bath was calibrated with a radium-beryllium source of known yield; (2) the bath was irradiated with the Li(p,n) source; from 1 and 2 the number of neutrons emitted per microcoulomb of protons striking the lithium target was computed; (3) fissions per microcoulomb were measured, in a separate run, from [redacted]

a 25 foil of known mass and area situated in an accurately known geometry with respect to the Li(p,n) source; and (4) the angular distribution of the neutrons from the Li(p,n) source was measured.

The fraction (β) of the total number of neutrons emitted by the Li(p,n) reaction that traversed the foil was determined from 4, and the known geometry of the 25 foil. Knowing the number of neutrons passing through the foil per microcoulomb of protons, the number of fissions per microcoulomb, the number of 25 atoms in the foil, and the area of the foil, the cross section for fission is given by (see Eq. 18, appendix)

$$\sigma_{25} = \frac{\text{fissions}/\mu c}{\beta Q} \qquad \frac{\pi r^2}{N_{25}} \tag{2}$$

Absolute fission cross sections were obtained at neutron energies of 250 Kev, 600 Kev and 1 Mev. More care was taken in determining the 1-Mev value since it is used as a standard and a considerable amount of effort has been made to determine it accurately. The angular distribution measurements from which the fraction of neutrons passing through the foil (β) was determined were made by Taschek and are given in Part I Table VII, of this report. Table VIII gives a summary of the data used in computing the cross sections and Table IX gives the cross section values for the various values of beta. The value of 1.33×10^{-24} cm^2 obtained for 1 Mev after making the 4.3% correction for leakage of Ra-Be neutrons from the tank checks the value obtained by Koontz[8].

APPENDIX

I. MANGANESE ACTIVITY VS. IRRADIATION TIME

Let R represent the number of activated manganese atoms produced per second in the bath by neutron capture, let N represent the number of activated atoms present at any time t, and let λ be the half life of Mn^{56}. Since $N\lambda$ is the rate of decay of

8) LA-128

Mn^{56} it is clear that the following relation applies:

$$dN/dt = R - N\lambda. \qquad (1)$$

The solution of this differential equation is,

$$N\lambda = R(1 - e^{-\lambda t}) = kA, \qquad (2)$$

where A is the observed manganese activity and k is a proportionality factor depending upon the counting geometry. It is clear that R, the rate of formation of activated atoms, depends upon the number of manganese atoms present, the capture cross section of manganese, and the neutron flux.

Since the half-life of Mn^{56} is 2.59 hours,

$$\lambda = \frac{0.693}{2.59 \times 60} = \frac{1}{224.2} \qquad (3)$$

Therefore,

$$kA = N\lambda = \frac{N}{224.2} = R(1 - e^{-t/224.2}) \qquad (4)$$

or the number of activated atoms present as a function of irradiation time is,

$$N = 224.2\ R(1 - e^{-t/224.2}) \qquad (5)$$

II. COMPARISON OF Li(p,n) AND Ra-Be SOURCES

From (4) we can write for the exposure of a Ra-Be source in the bath,

$$A_{Ra\text{-}Be} = kQ_{Ra\text{-}Be}(1 - e^{-t_1/224.2}) \qquad (6)$$

where $Q_{Ra\text{-}Be}$ is the number of neutrons per minute emitted by the source, t_1 is the duration of the exposure in minutes, $A_{Ra\text{-}Be}$ is the observed Geiger counting rate, and k is a different constant taking into account the proportionality between source strength and activation rate.

For a Li(p,n) exposure, let $Q_{Li(p,n)}$ be the number of neutrons emitted from the Li target per microcoulomb of protons. Since the Ra-Be source strength is given

[redacted] as the number of neutrons per minute, in order to compare the two, $Q_{Li(p,n)}$ must be multiplied by the number of microcoulombs per minute, i.e.,

$$Q_{Li(p,n)} \times \text{no. of microcoulombs per minute} = \text{no. of neutrons per minute} \quad (7)$$

Thus,

$$A_{Li(p,n)} = kQ_{Li(p,n)} \, (q/t_2) \, (1 - e^{-t_2/224.2}) \quad (8)$$

where q = microcoulombs of protons, and t_2 the exposure time in minutes. Taking the ratio of 6 to 8 we have,

$$\frac{A_{Ra-Be}}{A_{Li(p,n)}} = \frac{kQ_{Ra-Be}}{kQ_{Li(p,n)}} \times (q/t_2) \times \frac{(1 - e^{-t_1/224.2})}{(1 - e^{-t_2/224.2})} \quad (9)$$

or

$$Q_{Li(p,n)} = Q_{Ra-Be} \, \frac{A_{Li(p,n)}}{A_{Ra-Be}} \, \frac{t_2}{q} \, \frac{(1 - e^{-t_1/224.2})}{(1 - e^{-t_2/224.2})} \quad (10)$$

Normally the exposure time for the Li(p,n) source is quite short compared to that for the Ra-Be source. We see that (10) becomes indeterminate as $t_2 \to 0$ but evaluation of the indeterminate part gives,

$$Q_{Li(p,n)} = Q_{Ra-Be} \, \frac{A_{Li(p,n)}}{A_{Ra-Be}} \, \frac{224.2}{q} \, (1 - e^{-t_1/224.2}) \quad (11)$$

It is clear that $A_{Li(p,n)}$ and A_{Ra-Be} are the activities as measured by a Geiger counter with standard geometry at the time exposure is stopped (or at equal times thereafter). In my case the measured activities were always extrapolated back to zero time, i.e., the time exposure was stopped.

III. CALIBRATION OF BATH

In calibrating the bath with a Ra-Be source it is convenient to use the saturation activity or activity for infinite exposure time rather than the activity for some arbitrary time. For a given manganese concentration and source strength a [redacted]

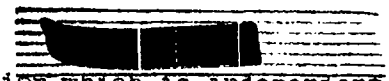

number is obtained by the calibration which is independent of exposure time.

From (6)

$$A_{Ra-Be}\ (t_1) = kQ_{Ra-Be}\ (1 - e^{-t_1/224.2}) \tag{12}$$

For saturation exposure, i.e., $t_1 \to \infty$,

$$A_{Ra-Be(saturation)} = kQ_{Ra-Be} \tag{13}$$

Taking the ratio of (12) and (13),

$$\frac{A(t_1)}{A(sat)} = (1 - e^{-t_1/224.2}) \tag{14}$$

or

$$A(sat) = \left(\frac{A(t_1)}{1 - e^{-t_1/224.2}}\right) \tag{15}$$

Substituting (15) in (11), we get,

$$\varphi_{Li(p,n)} = Q_{Ra-Be}\ \frac{A_{Li(p,n)}}{A_{Ra-Be\ (sat)}} \times \frac{224.2}{q}\ \frac{\text{neutrons}}{\text{microcoulomb}} \tag{16}$$

IV. FORMULA FOR CROSS SECTION

Let β denote the fraction of the total number of neutrons produced by the Li(p,n) reaction, which passes through the 25 foil. Then $\beta \times \varphi_{Li(p,n)}$ will be the number of neutrons per microcoulomb traversing the 25 foil. If N_{25} and σ_{25} are respectively the number of 25 atoms and the fission cross section then the total cross section is $N_{25}\sigma_{25}$ and the ratio of $N_{25}\sigma_{25}$ to the area of the foil (πr^2) will give the probability of a given neutron producing a fission. Hence

$$\frac{\text{no. of fissions}}{\text{no. of microcoulombs}} = \beta Q_{Li(p,n)} \times \frac{N_{25}\sigma_{25}}{\pi r^2} \tag{17}$$

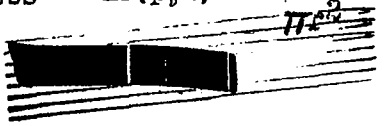

whence,

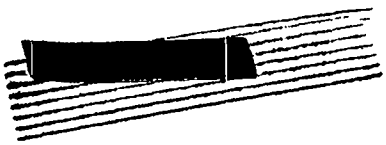

$$\sigma_{25} = \frac{(F/q)\,\pi r^2}{\beta Q_{Li(p,n)}\, N_{25}} \quad cm^2 \tag{18}$$

where F/q is the number of fissions per microcoulomb of protons.

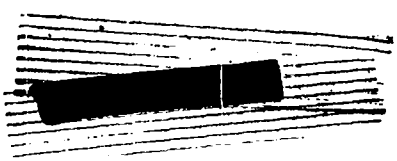

TABLE VIII

Summary of Data

Neutron Energy	Current Integral (Microcoulombs)	Manganese Activity counts/64/min	Fission Counts		Mn Activity per μcoul.	Fissions per μcoul.	Remarks
250 Kev	3938	26.7			0.00678		
250 Kev	5308	36.7			0.00692		
250 Kev	4534	32.8			0.00723		Discard-short tank on.
250 Kev	6186		1980			0.322	
250 Kev	6637		2410			0.363	
				Av	0.00685	0.342	
600 Kev	2501	47.4			0.01895		
600 Kev	2414	42.9			0.0177		
600 Kev	3160		4210			1.33	
600 Kev	3915		5450			1.39	
				Av	0.0183	1.36	
1 Mev	2339	33.3			0.01425		
	2285	32.4			0.0142		
	2651	36.7			0.01385		
	4163		3618			0.87	
	5573		4765			0.83	
				Av	0.0141	.85	

Ra-Be Saturation activity = 32.1 counts/64 /min.
Ra-Be Source No. 43.1000 calibration = 8.88×10^6 neutrons/sec
Foil Specifications:
Mass of 25 = 1.43 ± 0.03 mg.
Diameter = 3 cm

APPROVED FOR PUBLIC RELEASE

TABLE IX

Cross Sections

Neutron Energy	Mn activity per μcoul(av)	Fissions per μcoul(av)	Neutrons per μcoul	β (Table VII P+I)	σ	σ corrected for leakage
250 Kev	0.00685	0.342	2.55×10^{7}	1.90%	1.36×10^{-24} cm^2	1.43×10^{-24} cm^2
250 Kev				1.68%	1.54×10^{-24}	1.62×10^{-24}
250 Kev				1.64%	1.58×10^{-24}	1.66×10^{-24}
600 Kev	0.0183	1.36	6.82×10^{7}	2.77%	1.39×10^{-24}	1.46×10^{-24}
				2.70	1.42×10^{-24}	1.49×10^{-24}
1000 Kev	0.0141	0.85	5.25×10^{7}	2.50	1.27×10^{-24}	1.33×10^{-24}

APPROVED FOR PUBLIC RELEASE

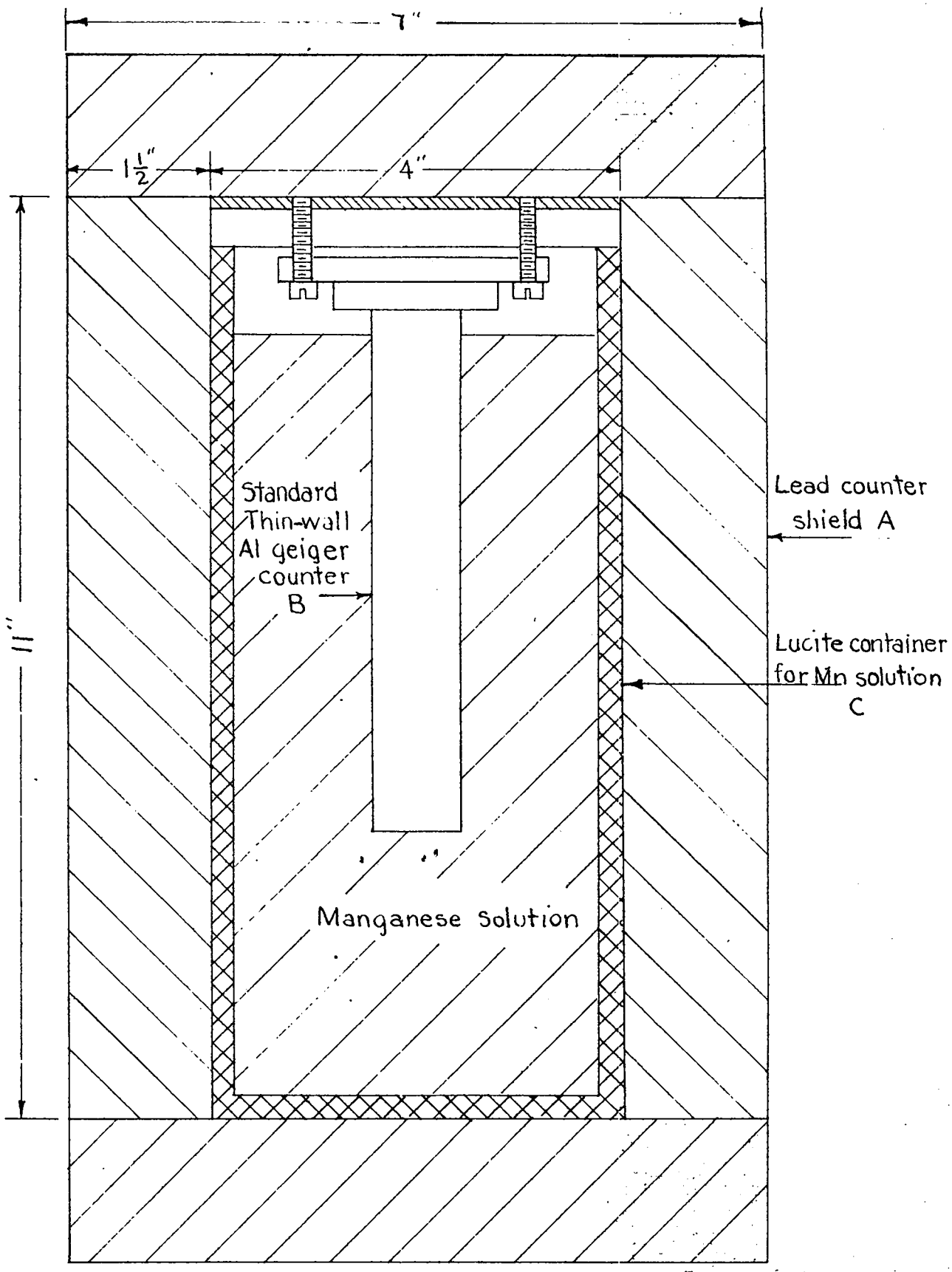

Fig. 7

GEIGER COUNTER ARRANGEMENT

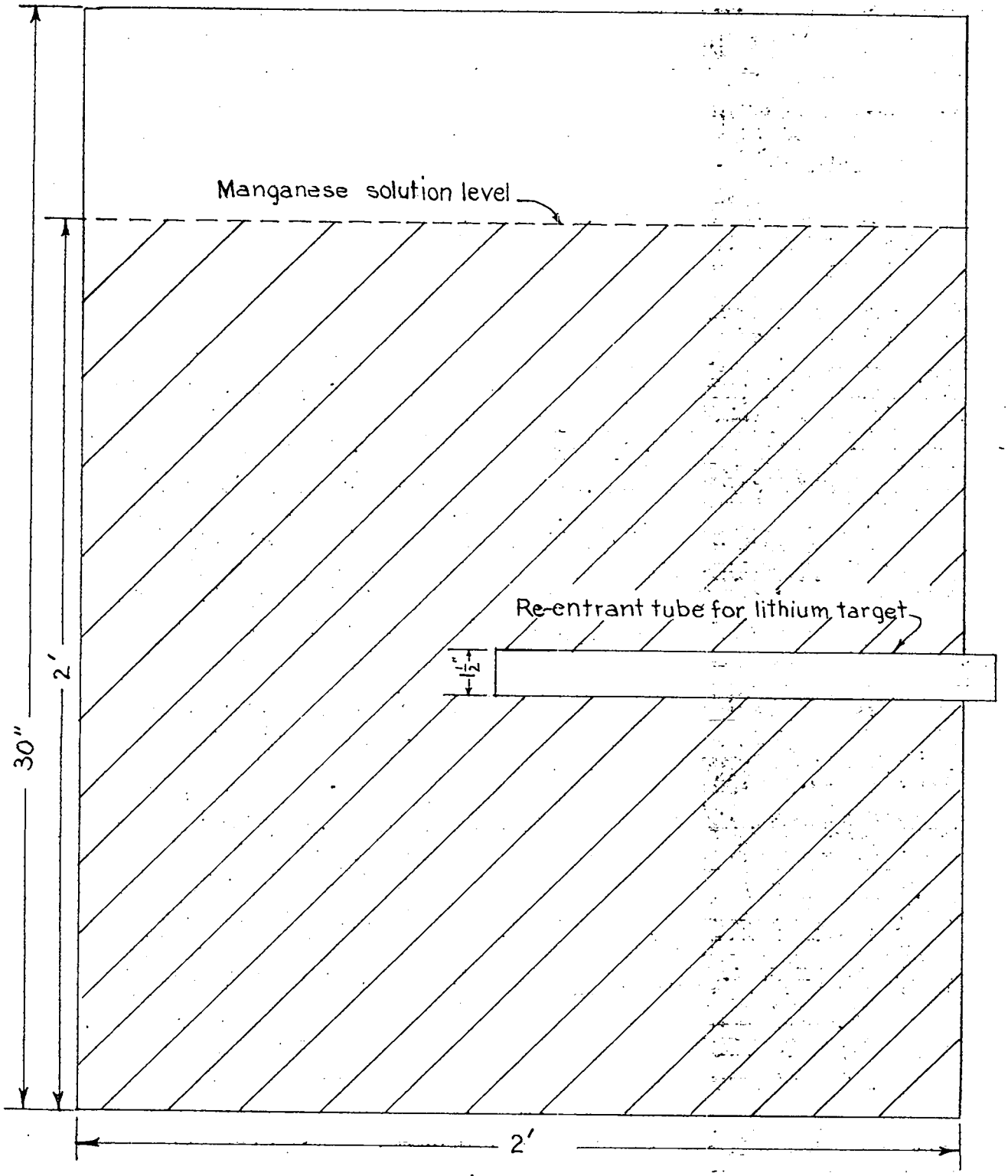

Fig. 8
MANGANESE BATH TANK

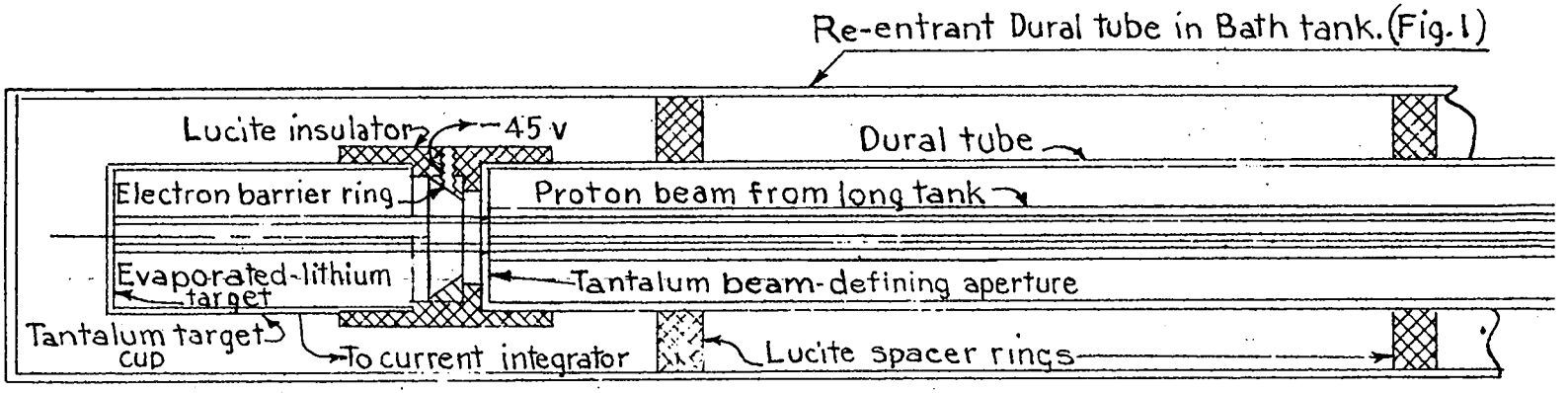

Fig. 9

LITHIUM TARGET ASSEMBLY FOR BATH

APPROVED FOR PUBLIC RELEASE

[redacted]